# Glucocorticoids preserve the t-tubular system in ventricular cardiomyocytes by upregulation of autophagic flux

## --- Supplementary Material ---

Thomas Seidel[1,2], Dominik J. Fiegle[1], Tim J. Baur[1], Anne Ritzer[1], Sandra Nay[1], Christian Heim[3], Michael Weyand[3], Hendrik Milting[4], Robert H. Oakley[5], John A. Cidlowski[5], Tilmann Volk[1,2]

[1] Institute of Cellular and Molecular Physiology, Friedrich-Alexander-Universität Erlangen-Nürnberg, Erlangen, Germany
[2] Muscle Research Center Erlangen (MURCE), Friedrich-Alexander-Universität Erlangen-Nürnberg, Erlangen, Germany
[3] Department of Cardiac Surgery, Friedrich-Alexander-Universität Erlangen-Nürnberg, Erlangen, Germany
[4] Erich & Hanna Klessmann Institute, Clinic for Thoracic and Cardiovascular Surgery, Heart and Diabetes Centre NRW, Ruhr-University Bochum, Bad Oeynhausen, Germany
[5] Signal Transduction Laboratory, Department of Health and Human Services, National Institute of Environmental Health Sciences, National Institutes of Health, Research Triangle Park, North Carolina, USA

## Detailed Methods

*Animals*

Female Wistar rats (150-200 g) were obtained from Charles River Germany. All experiments with rats were approved and performed according to the guidelines of the Animal Care and Use Committee Mittelfranken, Bavaria, Germany.

Female cardiomyocyte-specific glucocorticoid receptor knockout (GRKO) mice were generated and bred as described previously.[5, 6] All experiments with mice were approved and performed according to the guidelines of the Animal Care and Use Committee at the National Institute of Environmental Health Sciences (NIEHS), National Institutes of Health (NIH).

*Human cardiac samples*

Human cardiac tissue samples were collected from the left-ventricular apical core during implantation of mechanical assist devices (n=2) or from the free left-ventricular wall of explanted hearts (n=2). The study was approved by the institutional review boards, and all patients gave their written informed consent.

*Cardiomyocyte isolation*

Adult rat left-ventricular cardiomyocytes were isolated by Langendorff perfusion and enzymatic digestion as described elsewhere[3, 8]. Briefly, rats were deeply anesthetized by intraperitoneal injection of thiopental-sodium (100 mg/kg). Anaesthesia was verified by the absence of pain reflexes (firm toe pinch). After thoracotomy, hearts excised and retrogradely perfused with a modified Tyrode's solution, containing 1 µmol/L of free $Ca^{2+}$, collagenase (CLS type II, 160 U/mL, Biochrom) and protease (type XIV, 0.6 U/mL, Sigma). Myocytes from the left-ventricular free wall were then isolated by mincing and gently agitating the digested myocardium. Myocytes were stepwise adapted to physiological $Ca^{2+}$ levels and transferred to cell culture dishes containing culture medium. Human cardiomyocytes were isolated as described previously [14]. In brief, tissue samples were sliced, digested at 35˚ C for 10 min with 0.5 mg/ml protease XXIV (0.5mg/ml, Sigma) and with 1 mg/ml collagenase type I (Worthington) for 30-40 min. After dissociation, myocytes were gradually readapted to $Ca^{2+}$ and then transferred into culture dishes with culture medium.

*Cardiomyocyte culture*

After isolation, cardiomyocytes were either investigated immediately (fresh myocytes) or cultured for up to three days in M199 medium (Sigma, M4530) supplemented with 1 mg/mL bovine serum albumin (BSA, Roth, 0163.2) and penicillin/streptomycin (Biochrom, A2213) in cell culture dishes (Sarstedt, 83.3900) at 37˚ C, 80% relative humidity and 5% $CO_2$. In some experiments a modified Tyrode's solution, free from amino acids, was used as culture medium, containing in mmol/L NaCl 130, KCl 5.4, $MgCl_2$ 0.5, $NaH_2PO_4$ 0.4, glucose 22, HEPES 25, $NaHCO_3$ 5.8, $CaCl_2$ 2, supplemented with 1 mg/mL BSA, Penicillin/Streptomycin, and pH adjusted to 7.4[2]. Culture dishes were randomly assigned to treatment groups, including control (vehicle only, i.e. 0.01% ethanol or DMSO), 1 µmol/L dexamethasone (Sigma, D1756), 1 µmol/L corticosterone (Sigma, 27840), 10 µmol/L mifepristone (Sigma, M8046), 10 µmol/L spironolactone (Sigma, S3378), 0.1 µmol/L bafilomycin A1 (Invivogen, tlrl-baf1), 5 µmol/L chloroquine (Sigma, C6628), 1 µmol/L rapamycin (Sigma, R8781), 1 µmol/L verapamil (Spirochrome), 2 µmol/L nifedipine (Sigma, N7634), 10 nmol/L staurosporine (Sigma, S5921).

*Confocal imaging of living cardiomyocytes*

Living myocytes were placed into culture medium with 30 mmol/L butanedione monoxime (BDM, Sigma, B0753) and incubated with 8 µmol/L Di8-ANEPPS (Enzo LifeSciences, ENZ-52204) for 20 min at room temperature to stain cell membranes. Myocytes were then put into a microscope chamber and imaged with a Zeiss LSM 780 inverted confocal microscope, using a 63x oil immersion lens (NA 1.4). Di8-ANEPPS was excited by a 488 nm argon laser with depth-dependent increase in power[13], emission was recorded at 507-690 nm. Three-dimensional image stacks were acquired with a voxel size of $0.1\times0.1\times0.2$ µm$^3$ and image dimensions of $1280\times384\times50$ voxels, corresponding to $128\times38.4\times10$ µm$^3$. Pixel dwell time was set to 1.26 µs. Rod-shaped myocytes were randomly selected for image acquisition by light microscopy, with the researcher being blinded against treatment groups.

*Immunofluorescent staining and confocal imaging of fixed cardiomyocytes*

For immunostaining, cardiomyocytes were transferred to a 1.5 mL reaction tube, allowed to sediment at room temperature and then fixed with either 2% PFA for 5 min at room temperature (RyR, LTCC co-staining) or 100% acetone for 7 min at 4˚ C (BIN1,

JPH2 co-staining, LC3BII staining). After this and each of the following steps, a single washing step with cold PBS for 5 min was performed. For staining of t-tubule associated proteins, cells were incubated for 4-12 h at 4° C and protected from light with the primary antibodies against RyR2 (Thermo Fisher, MA3-916) and Cav1.2 (Alomone Labs, AGP-001), or BIN1 (Santa Cruz Biotechnology, sc23918) and JPH2 (Thermo Fisher, 40-5300), or LC3BII (Cell Signaling, 2775S), diluted 1:200 in PBS (acetone fixation) or PBS + 0.25% Triton X-100 (PFA fixation). Next, the secondary antibodies, goat anti-mouse AF488 (Thermo Fisher, A21121), goat anti-rabbit AF647 (Thermo Fisher, A32733) or goat anti-guinea pig AF555 (abcam, ab150186) and 4′,6-diamidino-2-phenylindole (DAPI) (Roth, 6335.1) were applied for 3 h at room temperature, diluted 1:200 in PBS, protected from light. For image acquisition, cells were transferred in PBS into a chamber with a coverslip bottom (thickness 1.5), mounted on the stage of a Zeiss LSM 780 inverted confocal microscope. Rod-shaped myocytes were randomly selected for image acquisition by light microscopy. Three-dimensional image stacks were acquired at the centre of the cell, using a 63x oil immersion lens (NA 1.4), voxel size of $0.1\times0.1\times0.2$ $\mu m^3$ and image dimensions of $1280\times384\times25$ voxels, corresponding to $128\times38.4\times5$ $\mu m^3$. Pixel dwell time was set to 1.26 µs. Excitation wavelengths were 405, 488 and 633 nm, emission filters were set to 415-480, 507-588, and 646-716 nm, respectively. Gain and laser power were adapted to avoid excessive photobleaching and saturation of signal intensities.

*$Ca^{2+}$ imaging*

Immediately after isolation or after culture, cardiomyocytes were transferred to modified Tyrode's solution, containing in mmol/L: 130 NaCl, 5.4 KCl, 0.5 $MgCl_2$, 0.4 $NaH_2PO_4$, 22 glucose, 25 HEPES, 2 $CaCl_2$, pH 7.4. Cell membranes were stained with 8 µmol/L Di8-ANEPPS and loaded with 10 µmol/L Fluo-4 AM (Thermo Fisher, F14217) and incubated at room temperature for 20 min before the experiment to de-esterify. Image acquisition was performed with a Zeiss LSM 780 inverted confocal microscope, using a 63x oil immersion lens (NA 1.4), a 488 nm argon laser for excitation, and emission filters set to 489-550 nm (Fluo-4) and 566-718 nm (Di8-ANEPPS). Pixel size was set to $0.1\times0.1$ $\mu m^2$. Images were acquired at approx. 21°C. Cells were stimulated with a field stimulation electrode powered by a stimulation device (MyoPacer EP, IonOptix, Westwood, USA) with 10-20 V biphasic pulses (pulse length 10 ms). Cells responding to stimulation were selected randomly by light microscopy

and then subjected to a standardized protocol. After adjusting the focal plane to the cell centre, the cell was stimulated for 30 s with 1 Hz prior to image acquisition. After a pause of 25 s, the myocyte was stimulated and a line scan simultaneously recorded in the cell centre along the myocyte long axis (1024 pixels, pixel dwell time 1.26 µs, sampling rate 529 Hz = 1.89 ms per line). For each data set, 2000 lines were scanned, corresponding to 3.78 s. Image acquisition and stimulation were synchronized with a Raspberry Pi single board computer, using a custom-written python script. Thereby, image acquisition started 500 ms before the cell was stimulated by a single biphasic pulse.

*Analysis of $Ca^{2+}$ signals*

Line scans were processed and analysed using a custom-written Matlab script (R2017b, Mathworks). First, the Fluo-4 and Di8-ANEPPS signals were noise-filtered with a mean filter of radius 3 in temporal and spatial dimension. Next, linear spillover from the Di8 into the Fluo-4 channel was detected and corrected, using a method described previously [11]. After spillover correction, the Fluo-4 signal (F) of each pixel was normalized to the mean signal intensity during diastole, using the first 200 ms of the data set ($F_0$). See Online Figure 12. Then, to obtain time of [$Ca^{2+}$] increase of the global $Ca^{2+}$ transient, the average of the whole line scan was calculated. A sigmoidal curve was fitted from baseline to $F_{max}$ and the time of maximum upstroke in Fluo-4 fluorescence intensity ($dF/dt_{max}$) identified. Time of $dF/dt_{max}$ was then determined for each pixel by fitting sigmoidal curves into the interval from 0 ms to the time of global [$Ca^{2+}$] increase +100 ms (see Online Figure 13 for an example). Using the Di8-ANEPPS signal, which was recorded in parallel, analysis was restricted to pixels within the cytosol. Cells with spontaneous contractions, movement artefacts or $F/F0_{max} < 1.5$ in all pixels were excluded. Movement artefacts were detected by correlating the Di8-ANEPPS signal of the first scanned line with all other lines. If the correlation coefficient fell below 0.5 before Ca transient rise time, this indicated spontaneous activity, and the cell was excluded from analysis. Also, individual pixels with $F/F0_{max} < 1.5$ were excluded (too low signal-to-noise ratio). $Ca^{2+}$ rise time was defined as time of $dF/dt_{max}$. Standard deviation of $Ca^{2+}$ release time was used to measure asynchrony of $Ca^{2+}$ rise. Line scan average Fluo-4 signals were used to calculate the time constant (tau) of the decay by fitting a mono-exponential function, starting at time of peak Fluo-4 signal.

*Sectioning and immunofluorescent staining of mouse cardiac tissue*

Floxed GR mice ($GR^{loxP/loxP}$) were generated and crossed with mice expressing Cre recombinase under the control of the alpha myosin heavy chain promoter (αMHCCre/+) as described[5, 6] to specifically delete the GR in cardiomyocytes. Hearts from 3-month old control and GRKO mice were frozen in liquid nitrogen and then stored at -80°C until usage. Frozen hearts were embedded in optimal cutting temperature (OCT) compound (Sakura FinetekEurope). Transverse sections of 60 µm thickness were cut on a cryotome (Leica, CM3050) at -20° C. The first 500 µm of the cardiac base and apex were excluded. For fixation, sections were promptly transferred to a 2% paraformaldehyde (PFA) solution dissolved in phosphate buffered saline (PBS, containing in mmol/L: 137 NaCl, 2.7 KCl, 10 $Na_2HPO_4$, 1.8 $KH_2PO_4$), incubated for 5 min and then washed in PBS. Antibodies against LTCC (Alomone, AGP-001) and RyR (Thermo Fisher, MA3-916) were diluted 1:200 in PBS containing 0.25% Triton X-100 and applied overnight at 4°C. After washing in PBS, secondary antibodies were incubated at 1:200 dilution for 5 h at room temperature, protected from light. For confocal microscopy, we used goat anti-mouse AF488 (Thermo Fisher, A21121) and goat anti-guinea pig AF555 (abcam, ab150186), for STED microscopy STAR 635P goat anti-guinea pig IgG (Abberior) and STAR 580 goat anti-mouse IgG (Abberior). For confocal microscopy, additional staining of nuclei with DAPI and of membranes and extracellular matrix with WGA-AF647 (Thermo Fisher, W32466) was applied. Sections were then embedded in Fluoromount G (Sigma, F4680) on a standard microscope slide, covered with a coverslip and dried at room temperature, protected from light, for at least 16 h before image acquisition.

*Confocal microscopy of mouse cardiac tissue*

From each cardiac cross section, three regions near the centre of the free left-ventricular wall were randomly selected by light microscopy. Image stacks of 1280×1280×150 voxels, corresponding to 128×1280×30 $\mu m^3$ (voxel size 0.1×0.1×0.2 $\mu m^3$) were recorded with the same microscope and imaging protocol as described for fixed rat cardiomyocytes. Laser power was increased with depth to compensate for signal attenuation.

*STED microscopy of mouse cardiac tissue*

For STED microscopy a 3D STED 2-channel super resolution system (Abberior, Göttingen, Germany) with an Olympus U-TB190 inverted microscope was used with a 100x oil immersion lens (numerical aperture: 1.44). Two pulsed laser lines (594 nm and 640 nm) were used for excitation, together with a high-power 775 nm laser (1250 mW) for emission depletion in 3D STED mode. Excitation filters HC615/25 and ET685/70 were used in laser lines 1 and 2, respectively. The emitted signal was detected with avalanche photo diode units. Pixel dwell time was 10 µs and voxel size was 0.03×0.03×0.038µm. Line accumulation was set to 2. The STED system was calibrated prior to imaging to achieve nearly spherical point-spread functions. FWHM of measured point spread functions (x×y×z dimension) was 0.11×0.13×0.19 $\mu m^3$ for the 594 nm channel and 0.15×0.20×0.21 µm for the 640 nm channel (Online Figure 15). For confocal image acquisition, the STED laser and line accumulation were disabled. Measuring point spread functions in confocal mode yielded FWHM of approx. 0.3×0.3×0.8 $\mu m^3$. Thus, the 3D STED mode improved planar and axial resolution by factors of approx. 2 and 4, respectively.

*Image processing and analysis*

All confocal and STED images were deconvolved using the Richardson-Lucy algorithm and measured point spread functions as described previously [7, 9]. Effects of deconvolution on images of TetraSpeck microspheres (Thermo Fisher, T729) are depicted in Online Figure 15. Image stacks of isolated cardiomyocytes were segmented into intracellular and extracellular space, using a semi-automated method based on morphological watersheds and iterative seed creation [12]. The intracellular space was morphologically closed and then used as a cell mask for all subsequent analyses. Immunofluorescent signals were separated from background by application of histogram-based thresholds: Mode ($m$) and standard deviation ($\sigma$) of images were calculated within the cell mask for each fluorescence channel. Thresholds were then set as follows: Di8-ANEPPS $m+1\sigma$, RyR $m+3\sigma$, JPH2 $m+3\sigma$, LTCC $m+3\sigma$, DAPI $m+4\sigma$, BIN1 $m+4\sigma$, LC3BII $m+3\sigma$, WGA $m+1\sigma$. The segmented Di8-ANEPPS signal corresponded to the cell membrane including the t-system and was further processed. First, the cell mask was used to separate the t-system from the surface sarcolemma. Morphological skeletonisation (thinning) then reduced t-tubule thickness to one pixel.

This minimized errors due to thresholding when calculating t-tubule density, which we defined as the number of t-system skeleton voxels divided by the number of intracellular voxels. The orientation angle of t-system components versus the myocyte long axis was calculated in three dimensions by vector gradient analysis [1, 14]. Clusters of RyR, JPH2, LTCC and LC3BII were detected by connected component analysis. From each component, the intensity-weighted centroid was determined and used to create Euclidean distance transforms, which in turn were used to perform nearest neighbour analyses, for example to measure RyR-LTCC distance.

*Patch Clamping*

The ruptured-patch whole-cell configuration was used as previously described[16]. Pipette resistance ranged from 2-5 MΩ. An EPC-10 amplifier (HEKA Elektronik, Lambrecht, Germany), controlled by the PULSE Software (HEKA Elektronik), was used. Membrane capacitance ($C_m$) and series resistance ($R_s$) were calculated using automated capacitance compensation. $R_s$ was < 10 MΩ in all experiments and was compensated by 85%, resulting in an average effective $R_s$ less than 1.5 MΩ. Pipette potentials were corrected for liquid junction potentials. Data were analysed using the PULSE-FIT software (HEKA Elektronik) and IGOR (WaveMetrics, Lake Oswego, OR, USA). All experiments were carried out at room temperature (20–22°C).

*Real-time qRT-PCR*

Fresh or cultured rat cardiomyocytes were collected in culture medium and centrifuged for 5 min at 1000×g. Cell pellets were immediately frozen at -80°C. RNA-isolation was performed using the NucleoSpin RNA-Kit from Macherey-Nagel, applying the given protocol for cells and tissue. RNA-concentration of each sample was measured with the Denovix DS 11+ spectrophotometer. Single-stranded cDNA was synthesized from 50 µg total RNA, using the QuantiTect reverse transcription kit from Quiagen. Quantitative real time PCR was carried out in the StepOnePlus cycler from Applied Biosystems, using the following sequence: 2 min at 50° C and 2 min at 95° C, then 40 cycles of 15 s at 95° C and 1 min 60° C and for the melt curve stage 15 s 95° C, 1 min 60° C and in 0.3°C steps to 95° C for 15 s.

The following intron-spanning primers were used:

| Gen | Primer 5´-3´ |
|---|---|
| BIN1 | fw: aaggcggatgaaacgaagga<br>rev: aagccaggtaggtccgaaga |
| JPH2 | fw: aggagtccaacattgcccgta<br>rev: gctctctgagttctccaggatct |
| GAPDH | fw: tgggaagctggtcatcaac<br>rev: gcatcaccccatttgatgtt |
| HPRT1 | fw: cccagcgtcgtgattagtga<br>rev: tcgagcaagtctttcagtcct |
| EEF2 | fw: aggccgccatgggtattaag<br>rev: aaggcatagaagcggccttt |

Specificity of primers was verified by gel electrophoresis and DNA sequencing following PCR. GAPDH, HPRT1 and EEF2 were amplified as an internal control. Samples were loaded in duplicates, and the results of each sample were normalized to the geometric mean of the control genes. Fold change was calculated as a ratio of treated over control.

*Western blotting*

Fresh or cultured rat cardiomyocytes were collected in culture medium and centrifuged for 5 min at 1000×g. Cell pellets were immediately frozen at -80˚ C. For protein isolation, cell pellets were resuspended in TNE-buffer (25 mmol/L Tris; pH 7.5; 150 mmol/L NaCl; 5 mmol/L EDTA; 1% Triton X-100) plus phosphatase inhibitor (PhosSTOP, Roche, 4906845001) plus phenylmethylsulfonylfluorid and lysed by sonification. Lysates were centrifuged for 5 min at 1000×g and the supernatant separated and put on ice. This step was repeated once, and the pooled supernatants were centrifuged for 2 h at 21,000×g at 4˚ C. Next, the supernatant was discarded and the pellet resuspended in TNE-buffer + 10% SDS + 1% Triton X-100. Subsequently, protein concentrations were determined by bicinchoninic acid (BCA) assay. For Western blotting, 10 or 20 µg of each sample were placed on acrylamide gels, and

electrophoresis was run for 1.5 h at 25 mV. Subsequently, proteins were transferred to a PVDF membrane (methanol-activated, 0.45µm pore size, Carl Roth, Karlsruhe, Germany) with a semi-dry blotting device (Trans Blot SD cell, Bio Rad, Hercules, USA) in blotting buffer (containing in mmol/L: 60 Tris, 50 glycine, 0.0016 SDS, and 20% V/V methanol) for 1h at 12 V. Membrane was blocked in blocking solution containing 5% low fat milk in Tris-buffered saline with 0.05% Tween (TBS-T) and then stained with the primary antibody. Following three washing steps with TBS-T, the secondary antibody, conjugated to horseradish peroxidase (HRP) was applied. Afterwards, the membrane was washed 3 times. This procedure was similar for all target proteins. See the table for details.

| **Target protein** | **Gel** | **Primary antibody** | **Secondary antibody** |
|---|---|---|---|
| BIN1 | 12% | Santa Cruz, sc-23918<br>1:500, 12h, 1% milk | abcam ab97023,<br>1:50000, 1h, 1% milk |
| CAV3 | 15 % | Santa Cruz, sc-5310<br>1:1000, 12h, 1% milk | abcam ab97023,<br>1:50000, 1h, 1% milk |
| GAPDH | 8-15% | Thermo Fisher, AM4300<br>1:20000, 1h, 1% milk | abcam ab97023,<br>1:50000, 1h, 1% milk |
| JPH2 | 8 % | Santa Cruz, sc-377086,<br>1:1000, 12 h, 1% milk | abcam ab97023,<br>1:50,000, 1 h, 1% milk |
| LC3B | 15% | Cell signalling, 2775S<br>1:1000, 12h, 1 % milk | Santa Cruz, sc-2054,<br>1:50000, 1h, 1% milk |
| SQSTM-1 (p62) | 12 % | Abcam, ab56416,<br>1:5000, 12 h, 1 % milk | abcam ab97023,<br>1:50,000, 1 h, 1% milk |

Finally, the membrane was incubated for 5 min in the dark with freshly prepared Super Signal West Femto solution (Thermo Fisher). Chemiluminescence was measured with a FusionSL Vilber Lourmat (Volber, Collegién, France). Saturation was avoided by adjusting exposure times of the camera. Dilution series verified that the applied amounts of protein were within the linear detection range of the antibodies and imaging system. Whole protein quantity was measured using Ponceau S staining solution

(Fluka BioChemika). Analysis was carried out with Fiji/ImageJ software[10]. At first, high-frequency noise was removed by Gaussian filtering (sigma 2). Next, local background was subtracted via the rolling ball method (white top-hat transform) with a radius of 50 pixels. This was also applied to photographs of Ponceau S staining. Finally, total signal intensity of bands of the target protein were measured and divided by the sum of signal intensity of several high-intensity Ponceau bands within the same lane, as described elsewhere.[4, 15] In addition to the control group from each cell isolation, each blot contained a control protein lysate, which was generated from aliquots of a large sample of freshly isolated rat cardiomyocytes. Normalization on this sample allowed for better comparison between blots.[15]

**Online Table 1**

| age | gender | surgery | HF type | etiology | EF [%] | LVEDD [mm] | secondary diagnoses |
|---|---|---|---|---|---|---|---|
| 51 | m | LVAD | HFrEF | DCM | 12 | 75 | arterial hypertenson, diabetes type II |
| 58 | m | LVAD | HFrEF | DCM | 20 | 58 | atrial fibrillation |
| 56 | m | HTX | HFrEF | DCM | 30 | 63 | arterial hypertension, atrial fibrillation, chronic kidney disease, |
| 63 | m | HTX | HFrEF | ICM | 25 | 69 | arterial hypertension, coronary artery disease, diabetes type II |

**Online Table 1.** Patient characteristics. Abbreviations: HF – heart failure, HFrEF – heart failure with reduced ejection fraction, DCM – dilatative cardiomyopathy, ICM – ischemic cardiomyopathy, EF – left-ventricular ejection fraction, LVEDD – left-ventricular end-diastolic diameter, LVAD – left-ventricular assist device, HTX – heart transplantation

## Online Figures

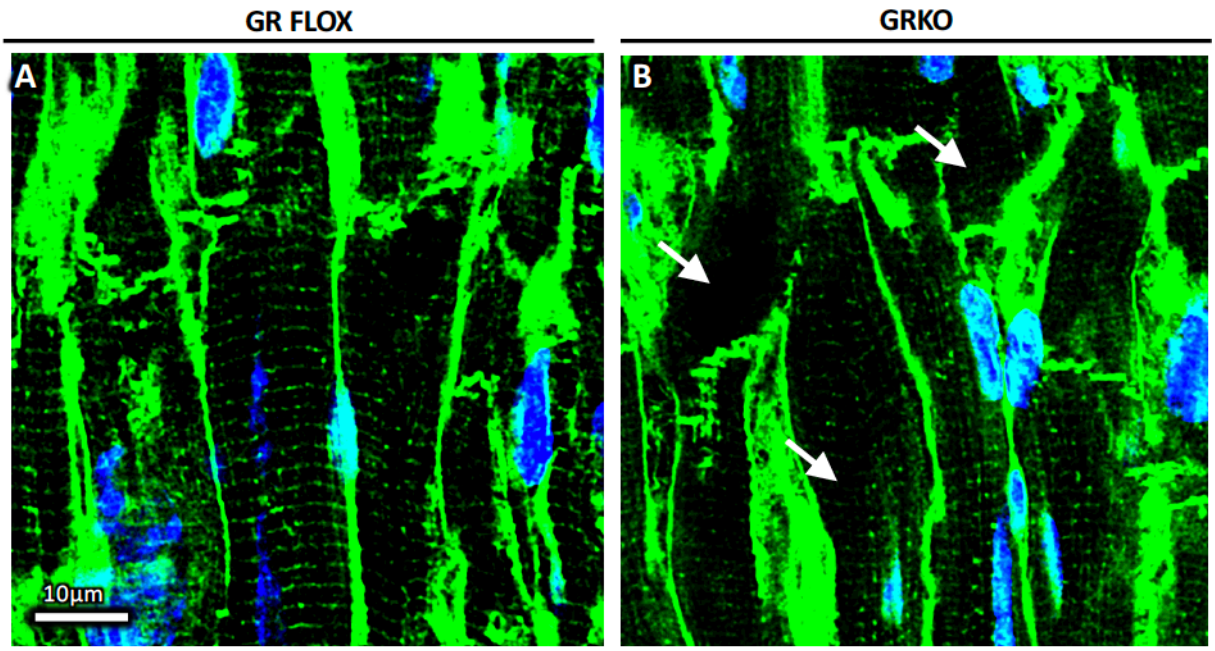


**Online Figure 1.** Confocal images of cardiac tissue sections from three-month old, **A,** control (GR FLOX) and, **B,** cardiomyocyte-specific GR knockout (GRKO) mice. Sections were stained with DAPI for nuclei (*blue*) and wheat germ agglutinin (WGA, *green*) for the sarcolemma, including t-tubules, and extracellular matrix. Arrows in *B* point to cell regions with weak or absent t-tubule staining.

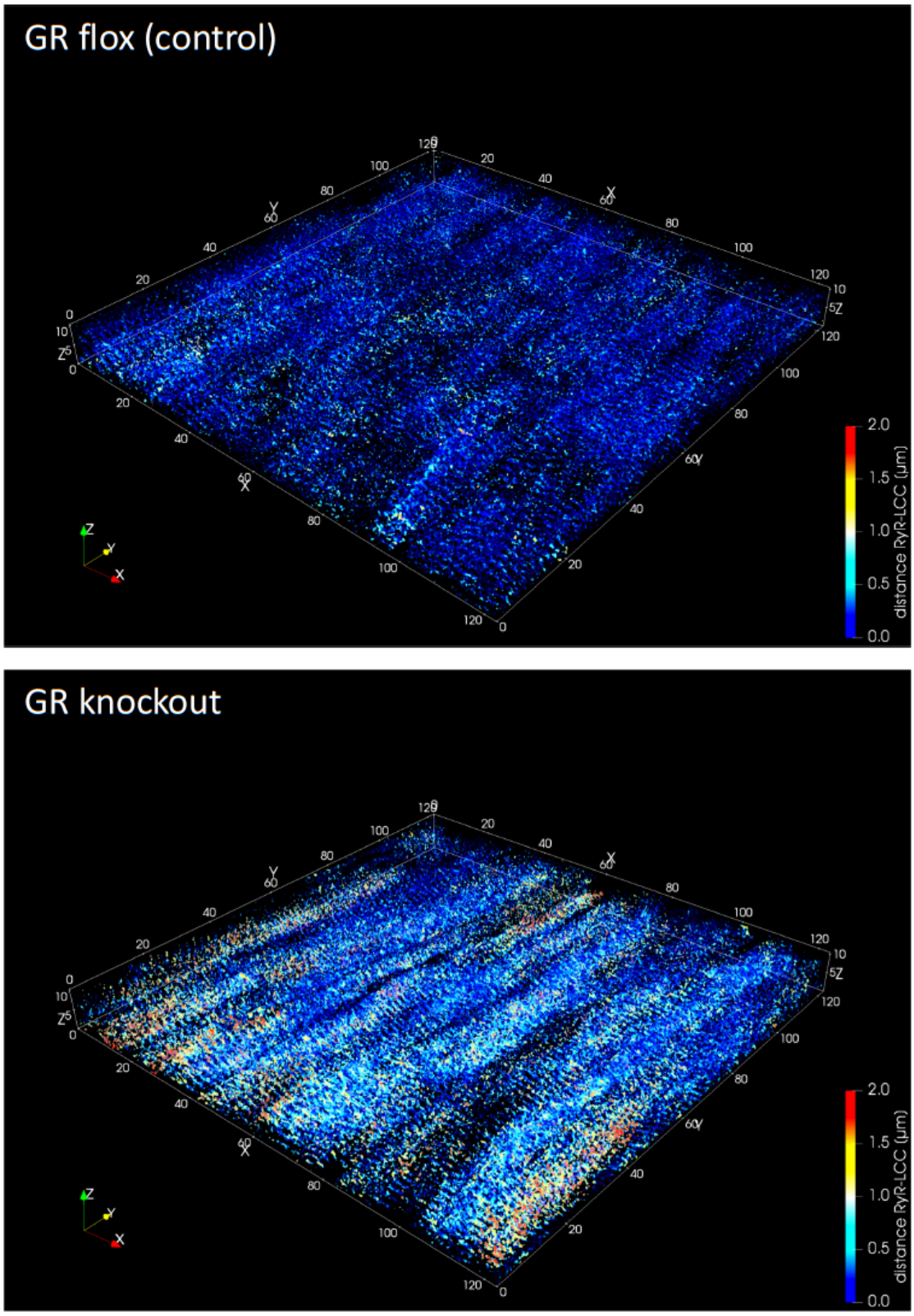


**Online Figure 2.** RyR cluster distances to closest L-type $Ca^{2+}$ channel (ΔRyR-LTCC) in tissue sections from control (top) and GR knockout mice (bottom). Dimensions of shown image stacks were 128×128×10 $\mu m^3$. See also the supplemental videos, showing animates views.

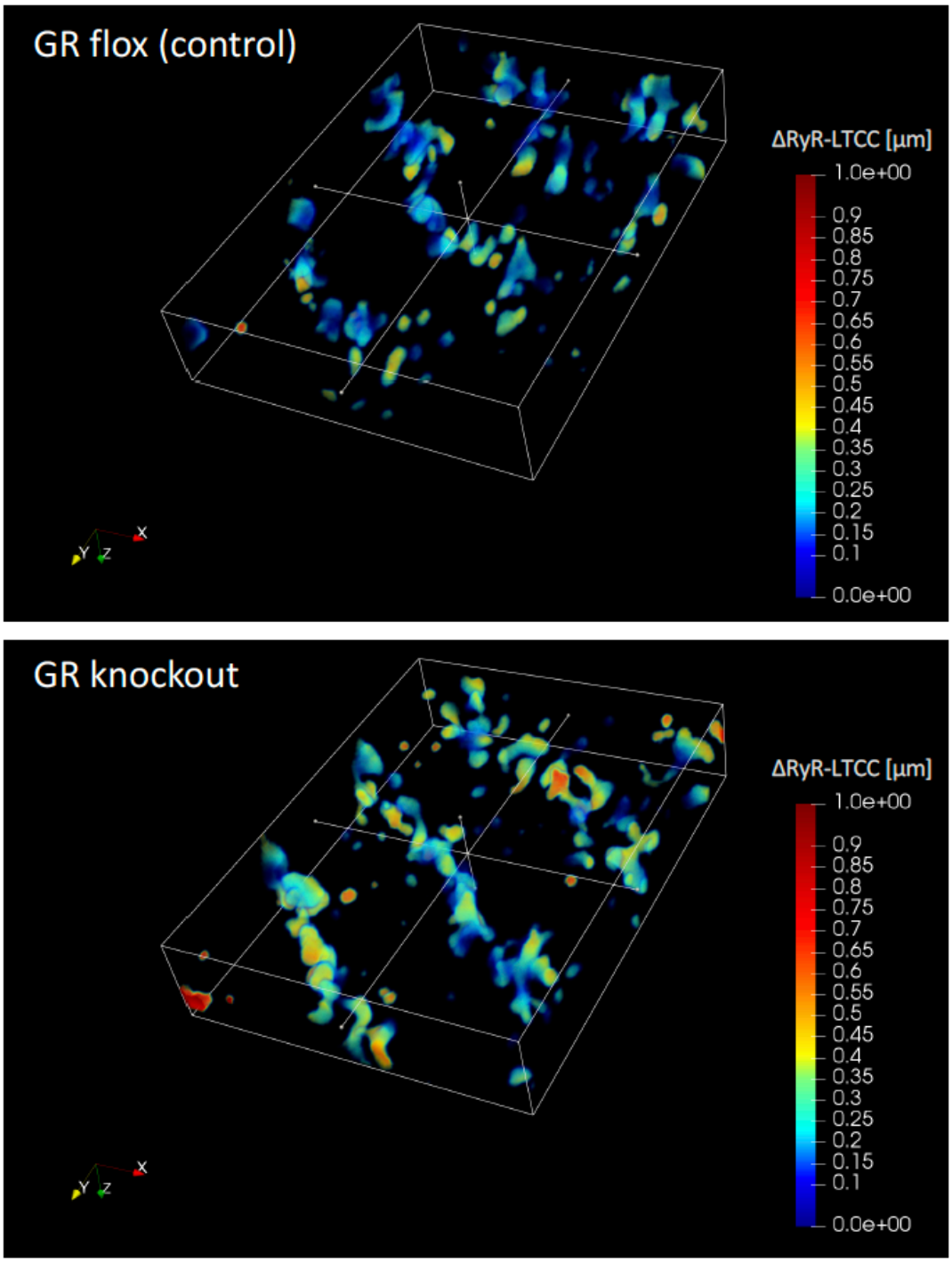


**Online Figure 3.** RyR cluster distances to closest L-type $Ca^{2+}$ channel (ΔRyR-LTCC) in tissue sections from control (top) and GR knockout mice (bottom), determined by 3D STED microscopy. Dimensions of shown image stacks were 6.6×6.6×3 $\mu m^3$. See also the supplemental videos, showing animates views.

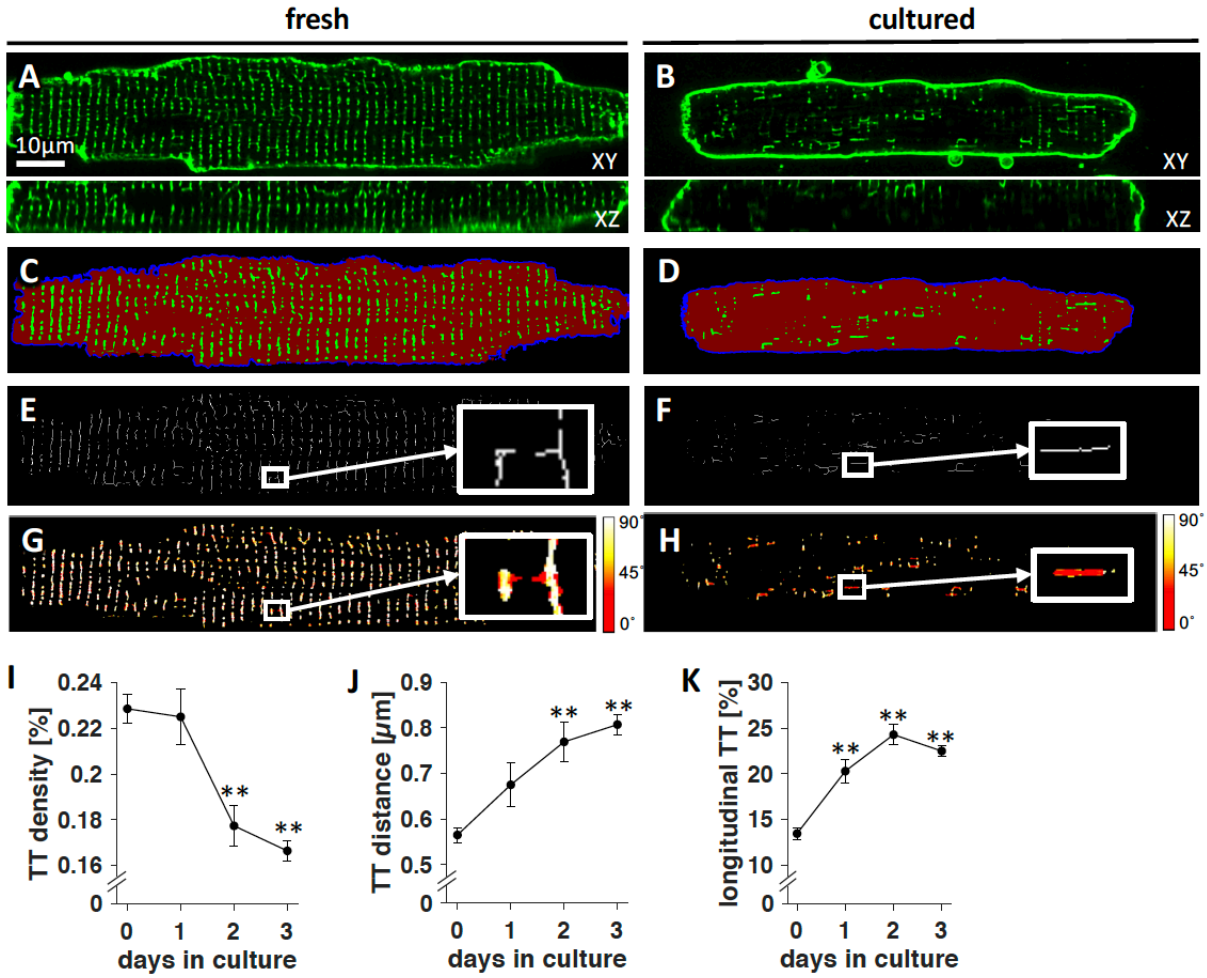


**Online Figure 4.** Imaging and analysis of the t-system in freshly isolated and cultured rat ventricular cardiomyocytes. **A and B,** Confocal images in XY and XZ views of Di8-ANEPPS-stained living myocytes directly after isolation (fresh) and after 3 days in culture (cultured). **C and D,** Corresponding cell masks (*dark red*) with t-system (*green*) and surface sarcolemma (*blue*), created by image segmentation. **E and F,** Skeleton, i.e. one-pixel-wide representation, of the t-system. **G and H,** Color-coded angles of t-system components versus x-axis, calculated in three dimensions. Insets show zoom-ins of boxed regions. **I**, Volume density of t-tubule skeleton (TT density), **J,** mean intracellular distance to nearest t-tubule (TT distance), and, **K,** fraction of longitudinal (angle<45˚) t-tubule components (longitudinal TT) in fresh myocytes (0d) and cells cultured for 1-3 days. Scale bar in *A* also applies to *B-H*. **p<0.01 vs fresh cells (two-tailed Welch's t-test), n (cells/animals) = 131/16, 65/9, 119/18, 492/60 in fresh, 1d, 2d and 3d cultured cells, respectively.

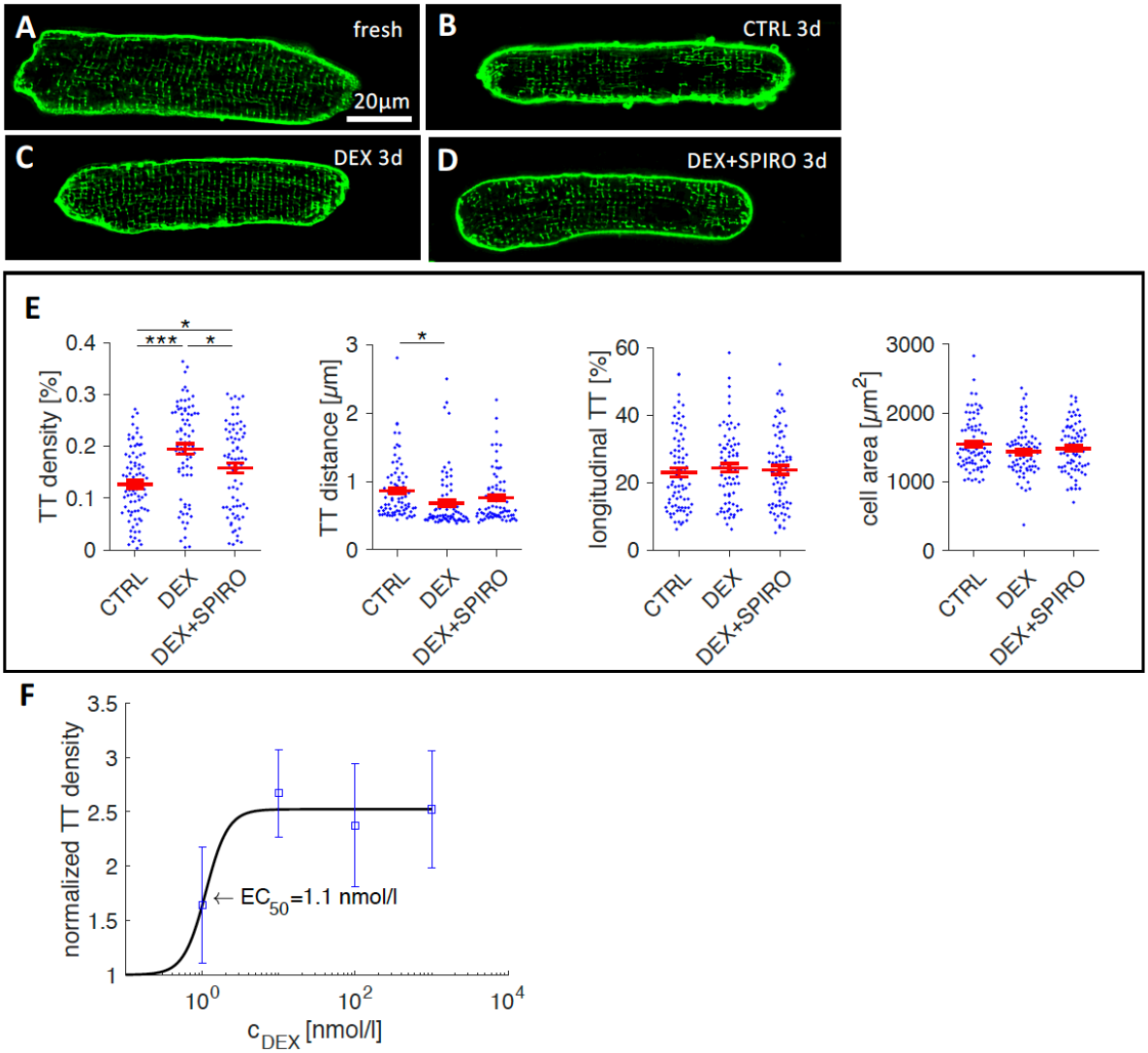


**Online Figure 5.** Effect of corticosteroid agonists and antagonists on the t-system in cultured rat cardiomyocytes. **A-D,** Confocal images of Di8-ANEPPS-stained living myocytes of (A) fresh cells and cells after 3d of culture treated with (B) vehicle (CTRL 3d), (C) 1 µmol/L dexamethasone (DEX 3d), (D) 1µmol/L dexamethasone + 10µmol/L spironolactone (DEX+SPIRO). Scale bar in A also applies to B-D. **E,** T-tubule density (TT density), mean intracellular distance to nearest t-tubule (TT distance), fraction of longitudinal t-tubule components (longitudinal TT), and cell area at cell centre in CTRL 3d, DEX 3d, and DEX+SPIRO 3d cells from matched cell isolations. *** $p<0.001$, *$p<0.05$, n (cells/animals) = 81/10, 76/10, 76/10 in CTRL 3d, DEX 3d and DEX+SPIRO 3d, respectively. **F,** Fitted dose-response curve of dexamethasone on t-system density after 3 days of culture, normalized to cultured CTRL cells from matched cell isolations (n=37-40 cells per group from 5 animals, error bars represent standard deviation)

**A**

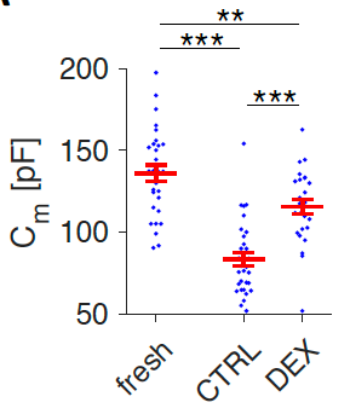


**B**

| | capacitance |
|---|---|
| fresh | 136±5 pF (n=29) |
| CTRL 3d | 83±4 pF (n=31) |
| DEX 3d | 115±5 pF (n=26) |

**Online Figure 6.** Effect of dexamethasone on cell capacitance in cultured rat cardiomyocytes. **A,** Mean capacitance measured by whole-cell patch clamping technique in freshly isolated (fresh) myocytes and cultured myocytes treated for 3 days with vehicle (CTRL) or 1 µmol/L dexamethasone (DEX). **B,** Representation as table. Cells were obtained from 8 cell isolations. *** p<0.001, **p<0.01

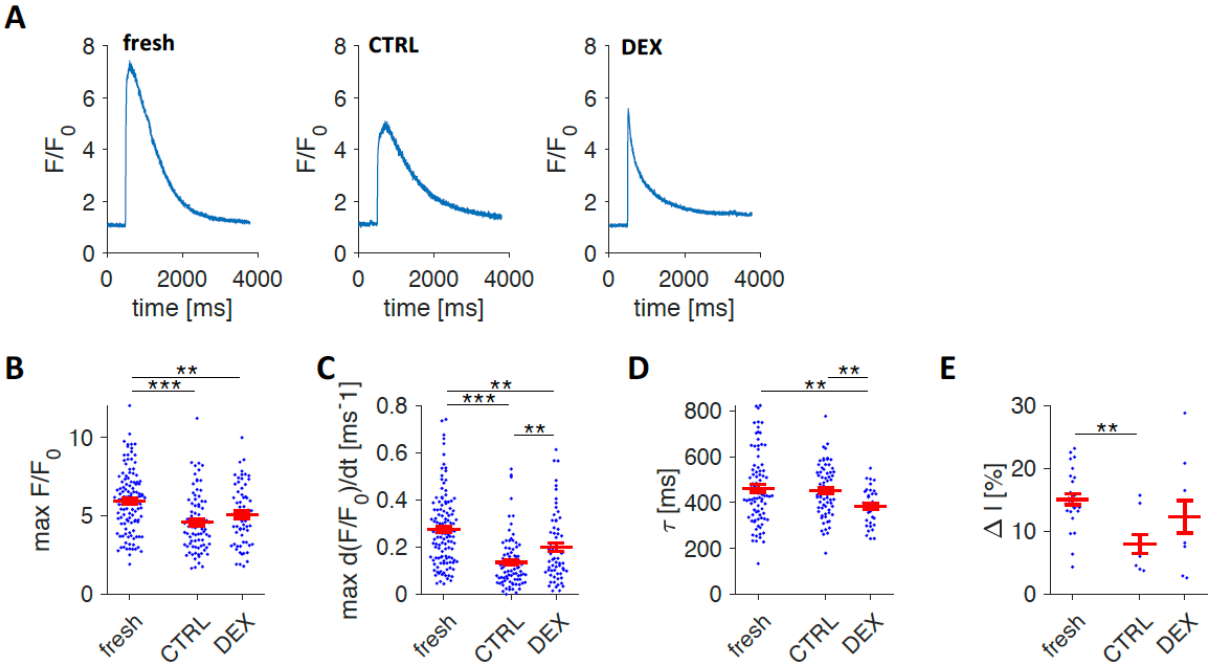


**Online Figure 7.** Effect of culture with or without dexamethasone treatment on $Ca^{2+}$ transient kinetics in rat cardiomyocytes. Freshly isolated myocytes (fresh) and myocytes cultured for 3 days in vehicle (CTRL) or 1µmol/L dexamethasone (DEX) were stained with Di-8-ANEPPS, loaded with Fluo-4-AM as Ca2+ indicator and then scanned with confocal microscopy during field stimulation at room temperature. Mean Fluo4 signals of line scans were analyzed to obtain kinetics (A-C). Di8 signal was analyzed with edge detection to obtain contraction (D). **A,** Representative examples of Fluo4 signal normalized to baseline signal intensity before stimulation (F/F0) from fresh, DEX and CTRL cells, **B,** Maximum (amplitude) F/F0, as indicator of maximum cytosolic $Ca^{2+}$ concentration. **C,** Maximum increase of Fluo4 signal (maximum of d(F/F0)/dt), as indicator of maximum cytosolic $Ca^{2+}$ influx. **D,** Time constant ($\tau$) of exponentially fitted decay of Fluo4 signal, as indicator of cytosolic $Ca^{2+}$ efflux. **E,** Maximum relative change in cell length ($\Delta$l) during contraction. Note that only cells with both longitudinal ends within the scanned line were analyzed. ***p<0.001, **p<0.01, *p<0.05, n (cells/animals) n = 122/11, 83/8, 66/8 (B-D) and 27/10, 9/3, 10/3 (E) in fresh, CTRL3d, DEX3d, respectively. Two-tailed Welch's t-test was used for all tests, with multiple comparison correction.

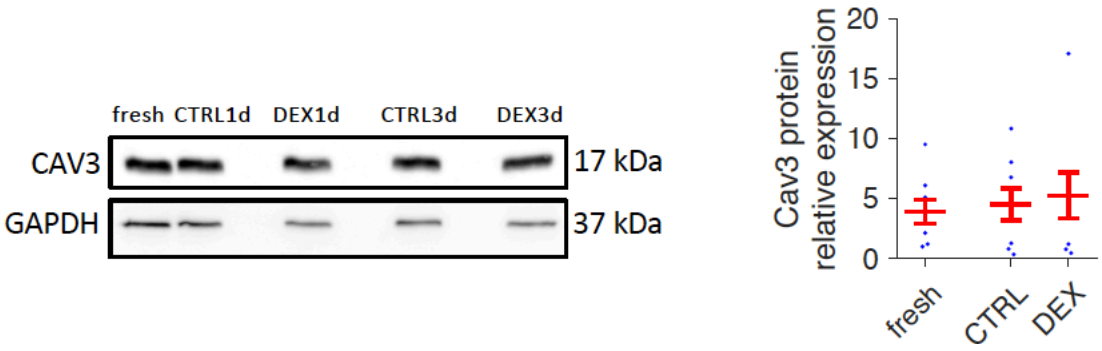


**Online Figure 8.** CAV3 protein expression assessed by Western blotting. Quantification (normalization by Ponceau staining) in fresh cells and cells cultured for three days treated with vehicle (control, CTRL) or 1 µmol/L dexamethasone (DEX). n = 8 matched cell isolations

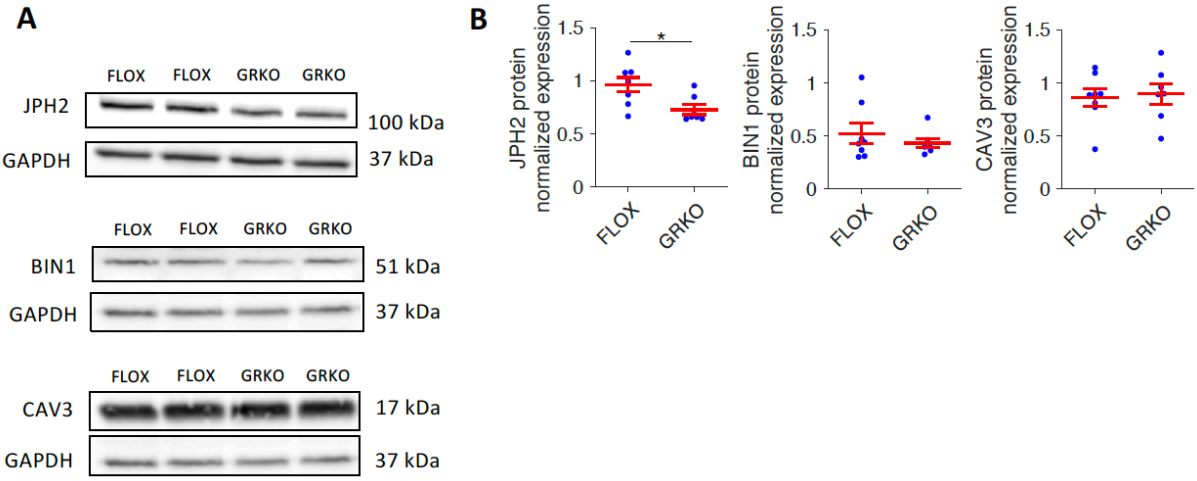


**Online Figure 9.** Junctional proteins in cardiomyocyte-specific glucocorticoid receptor knockout (GRKO) and control (FLOX) mice. **A,** Examples and **B,** quantification of Western blots for JPH2, bridging integrator-1, and caveolin-3 (CAV3) in FLOX and GRKO samples. Band intensities were normalized to Ponceau staining and a reference sample. n=8/7 in FLOX/GRKO, respectively. * indicates $p<0.05$ from Welch‘s t-test.

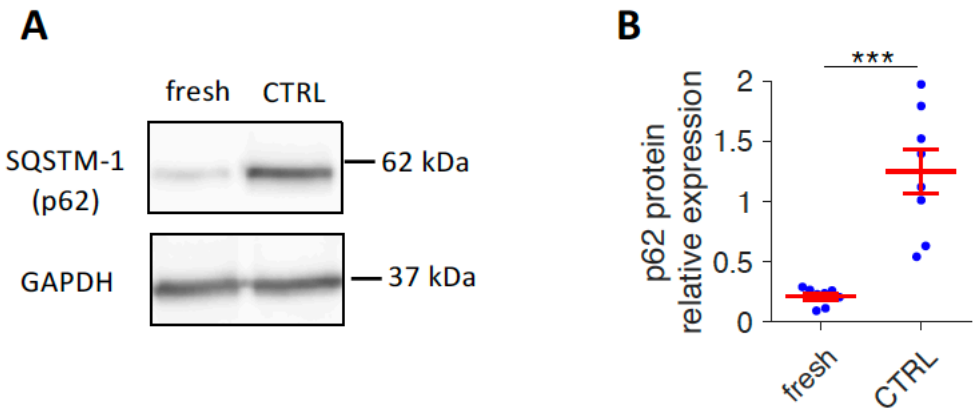


**Online Figure 10**. Effects of cell culture on SQSTM-1 (p62) protein expression rat cardiomyocytes. **A,** Example, and **B,** Quantitative analysis of SQSTM-1 (p62) Western blots from freshly isolated myocytes (fresh) and myocytes cultured for 1d under control conditions (CTRL). n = 8 matched cell isolations. Protein expressions were quantified by normalization to Ponceau staining and a reference sample. **p<0.01 (paired t-tests)

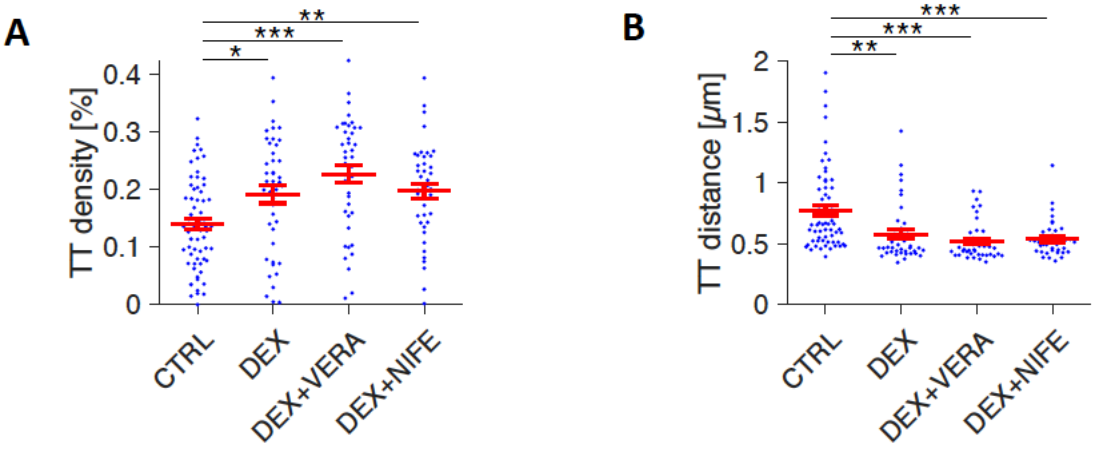


**Online Figure 11.** Effect of calcium channel antagonists on t-system preservation by dexamethasone in cultured rat cardiomyocytes. **A,** T-tubule density (TT density), **B,** mean intracellular distance to nearest t-tubule (TT distance), in cells treated for three days with vehicle (CTRL), 1 µmol/L dexamethasone (DEX), 1 µmol/L dexamethasone + 1 µmol/L verapamil (DEX+VERA) or 1 µmol/L dexamethasone + 2 µmol/L nifedipine (DEX+NIFE) from matched cell isolations. ***p<0.001, **p<0.01, *p<0.05, n (cells/animals) = 64/6, 43/6, 42/6, 42/6 in CTRL, DEX, DEX+VERA, DEX+NIFE, respectively.

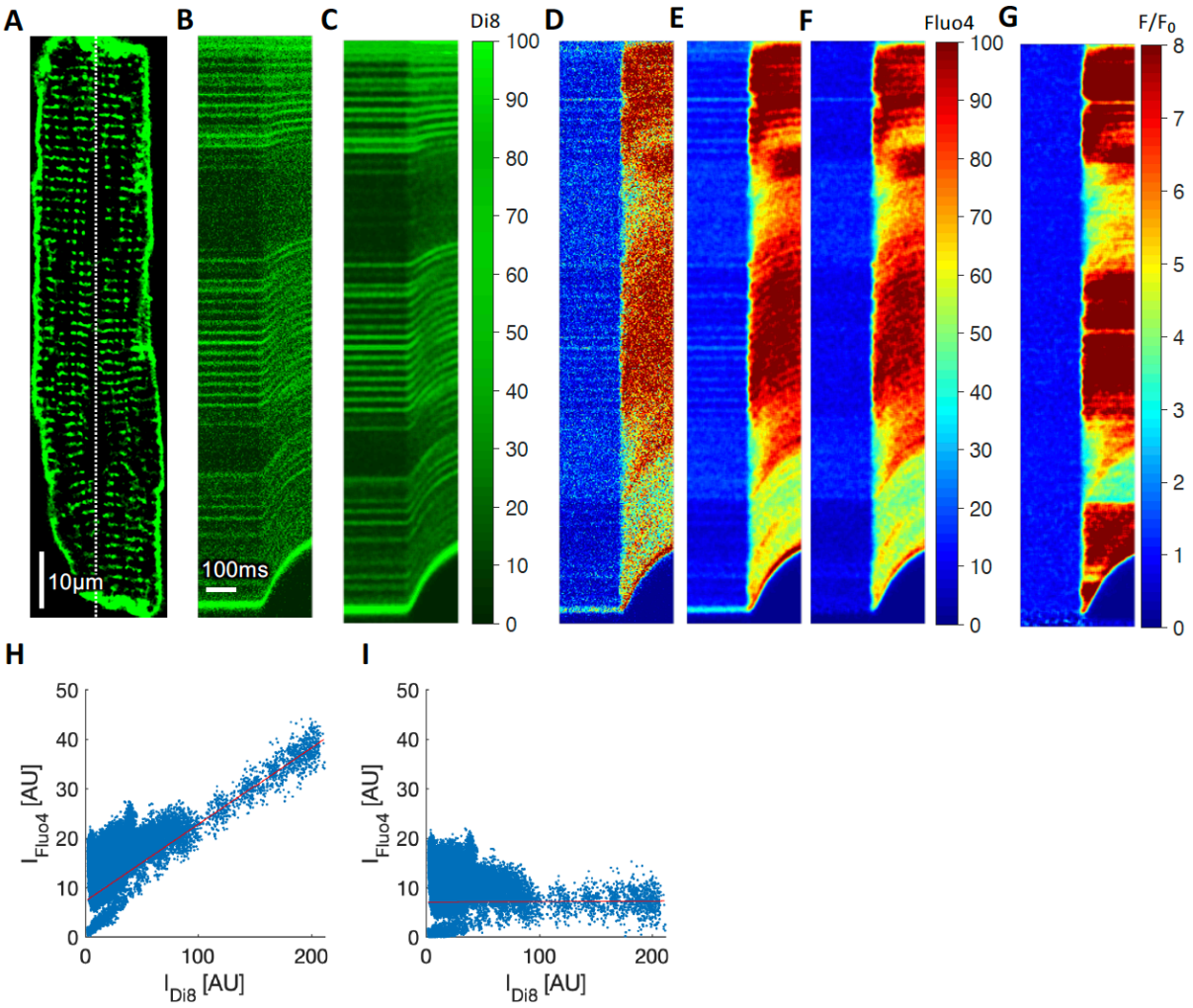


**Online Figure 12.** Preprocessing of confocal line scans. **A,** 2D scan of example myocyte stained with Di8-ANEPPS (Di8, *green*). White dots indicate the scanned line. **B,** Raw Di8 signal of line scan. **C,** Noise-filtered Di8 signal. **D,** Raw Fluo4 signal. **E,** Noise-filtered Fluo4 signal. **F,** Noise-filtered Fluo4 signal after spillover correction. **G,** Fluo4 signal normalized to baseline intensity before stimulation ($F/F_0$). **H,** Correlation of Di8 signal intensity ($I_{Di8}$) with Fluo4 signal intensity ($I_{Fluo4}$) before spillover correction (pixel intensities from filtered signals before stimulation). The slope of the red line indicates the correlation coefficient (r=0.155). **I,** Correlation of $I_{Di8}$ with $I_{Fluo4}$ after spillover correction (r=0.001). Scale bar in A also applies to B-G. Scale bar in B also applies to B-G

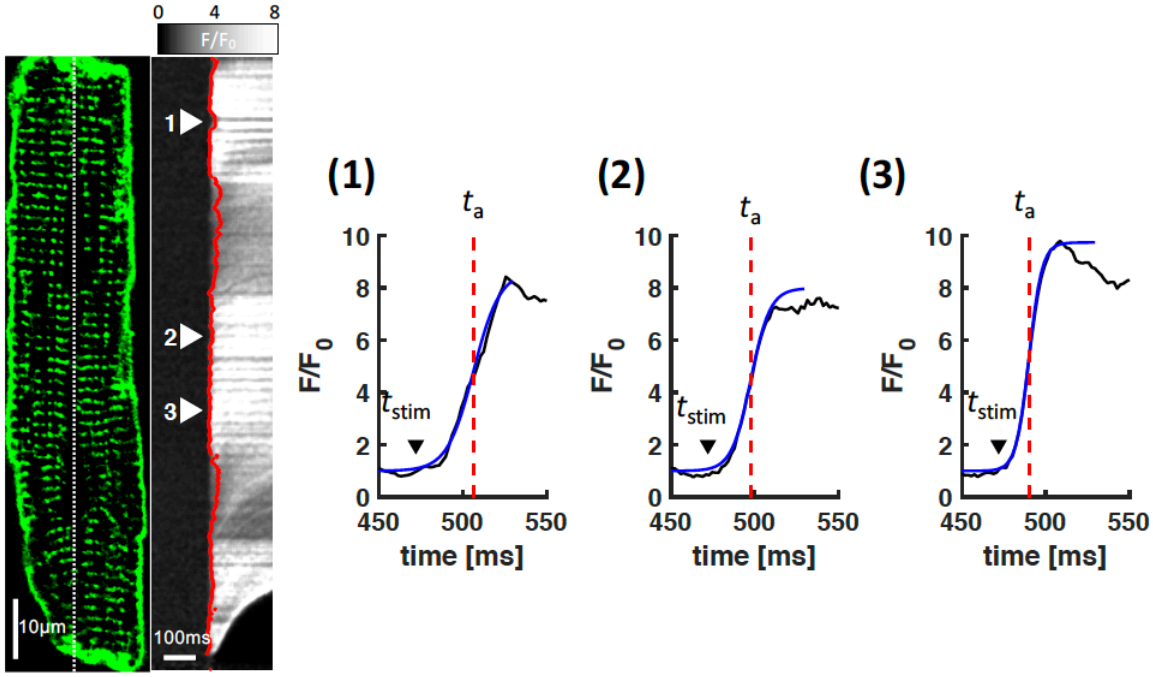


**Online Figure 13.** Analysis of activation times of $Ca^{2+}$ release ($t_a$) in confocal line scans of isolated rat cardiomyocytes. The picture on the left shows a 2D confocal image of a myocyte stained with Di8-ANEPPs (green) and the line subsequently scanned during $Ca^{2+}$ imaging (dashed line). Cells were field-stimulated 472 ms after start of image acquisition ($t_{stim}$) and Fluo4 signals recorded with 1.89 ms per line. Traces of the three points marked by white arrowheads are shown on the right. The median-filtered signal, normalized to baseline ($F/F_0$) is shown in black, the fitted curve in blue. Detected $t_a$, defined as maximum upstroke of $F/F_0$ in the fitted curve, is indicated by red dashed lines.

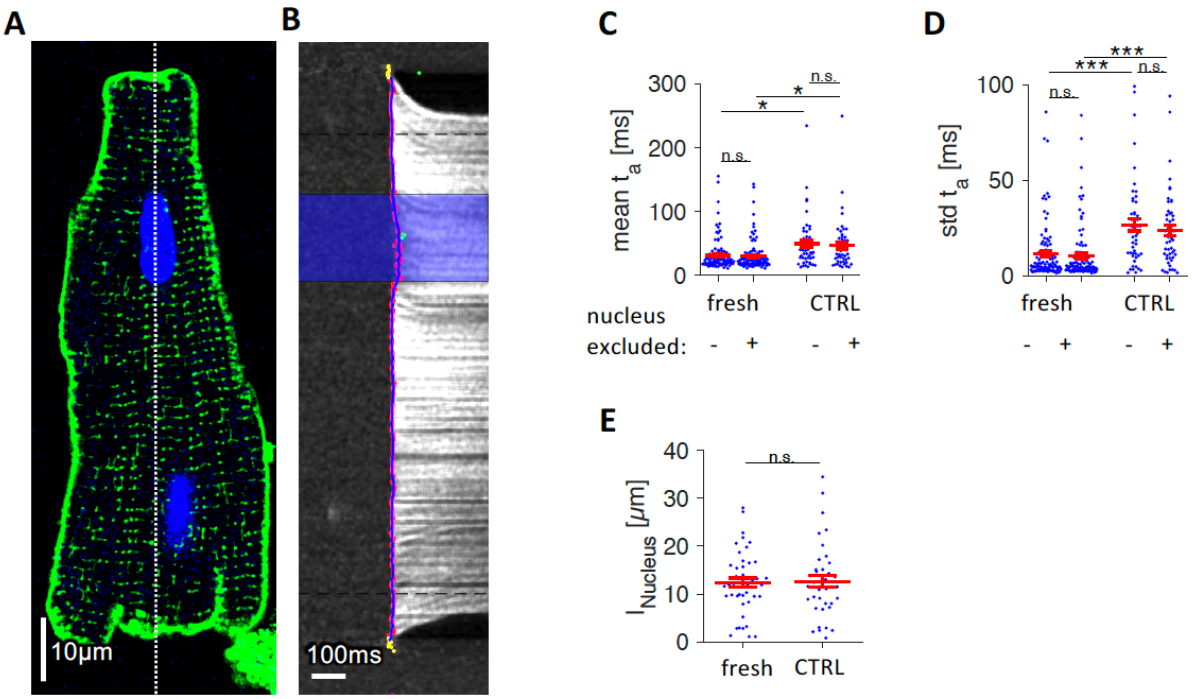


**Online Figure 14.** Effect of nucleus exclusion on $Ca^{2+}$ transient analyses in fresh and cultured rat cardiomyocytes. **A,** 2D scan of exemplary fresh myocyte stained with Di8-ANEPPS (Di8, *green*) and Hoechst 33342 (*blue*). White dots indicate the scanned line. **B,** Corresponding normalized Fluo4 signal ($F/F_0$, *gray*) acquired by line scan. The blue area indicates the nucleus position. Times of maximum $F/F_0$ upstroke velocity (activation time, $t_a$) are indicated as red pixels. The blue line next to red pixels indicates a moving mean (window size: 2.5µm) of $t_a$. Yellow pixels were excluded (SNR < 1.5). Green pixels indicate statistical outliers (> 5x interquartile range). **C,** Mean, and **D,** Standard deviation (std) of $t_a$, calculated either from all pixels (nucleus not excluded, -) or from cytosolic pixels only (nucleus excluded, +) in fresh myocytes or myocytes cultured for 3 days under control conditions (CTRL). **E,** Length of line occupied by nucleus ($l_{Nucleus}$) ***p<0.001, **p<0.01, *p<0.05, n (cells/animals) = 104/8, 51/4 in fresh and CTRL respectively. Two-tailed Welch's t-test was used for all tests, with multiple comparison correction. Scale bar in A also applies to B.

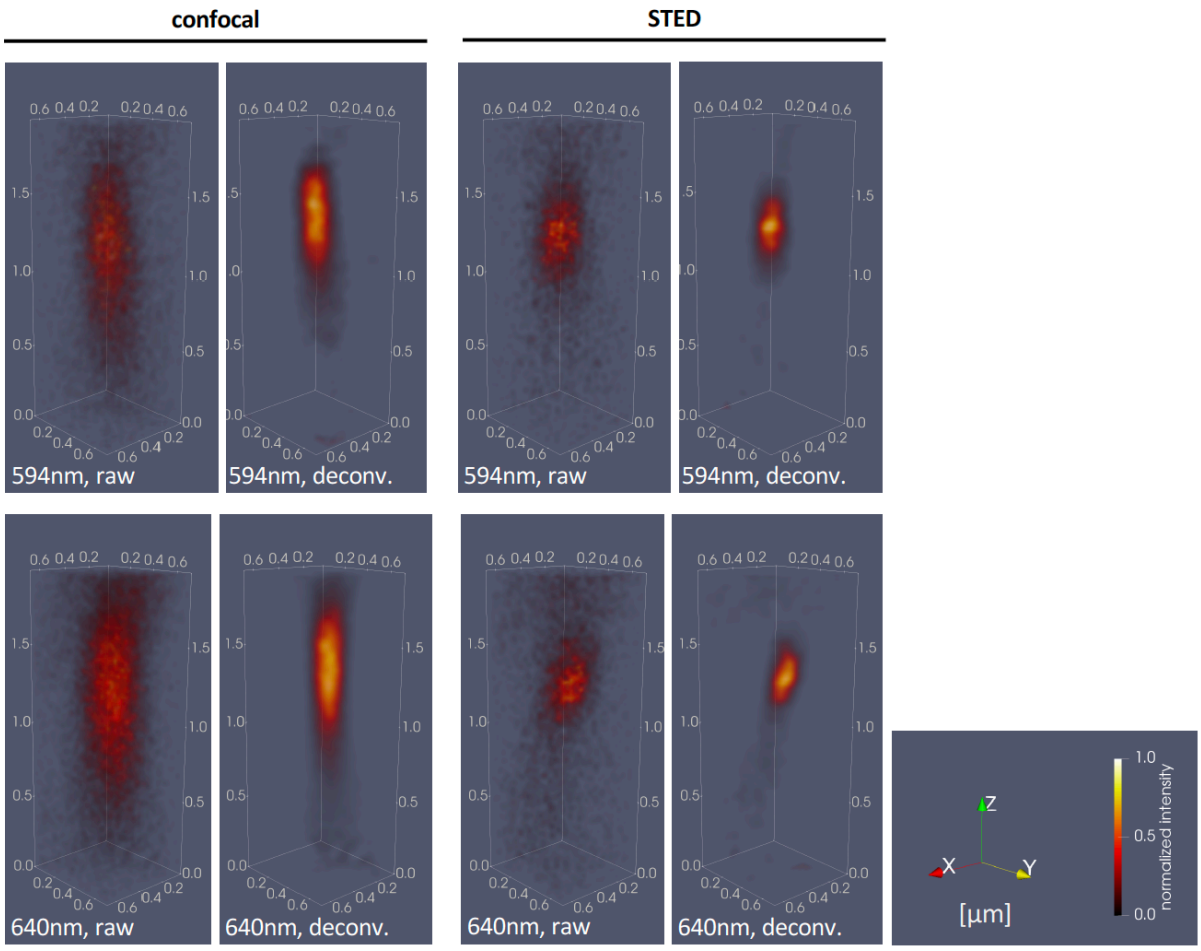


**Online Figure 15.** Tetra specs (radius 50 nm) imaged with confocal and 3D STED microscopy, using the 594nm (top) or 640 nm laser (bottom). Images shown represent signals before (raw) and after deconvolution with measured point spread functions (deconv.).

## References


1. Bauer C, Bischof H (2008) A Novel Approach for Detection of Tubular Objects and Its Application to Medical Image Analysis. In: Lecture Notes in Computer Science. Springer, p 163-172
2. Benitah JP, Vassort G (1999) Aldosterone upregulates Ca(2+) current in adult rat cardiomyocytes. Circ Res 85:1139-1145
3. Foltz WU, Wagner M, Rudakova E, Volk T (2012) N-acetylcysteine prevents electrical remodeling and attenuates cellular hypertrophy in epicardial myocytes of rats with ascending aortic stenosis. Basic Res Cardiol 107:290 doi:10.1007/s00395-012-0290-4
4. McDonough AA, Veiras LC, Minas JN, Ralph DL (2015) Considerations when quantitating protein abundance by immunoblot. Am J Physiol Cell Physiol 308:C426-433 doi:10.1152/ajpcell.00400.2014
5. Oakley RH, Cruz-Topete D, He B, Foley JF, Myers PH, Xu X, Gomez-Sanchez CE, Chambon P, Willis MS, Cidlowski JA (2019) Cardiomyocyte glucocorticoid and mineralocorticoid receptors directly and antagonistically regulate heart disease in mice. Sci Signal:in press
6. Oakley RH, Ren R, Cruz-Topete D, Bird GS, Myers PH, Boyle MC, Schneider MD, Willis MS, Cidlowski JA (2013) Essential role of stress hormone signaling in cardiomyocytes for the prevention of heart disease. Proc Natl Acad Sci U S A 110:17035-17040 doi:10.1073/pnas.1302546110
7. Richardson WH (1972) Bayesian-Based Iterative Method of Image Restoration*. J. Opt. Soc. Am. 62:55-59 doi:10.1364/JOSA.62.000055
8. Rudakova E, Wagner M, Frank M, Volk T (2015) Localization of Kv4.2 and KChIP2 in lipid rafts and modulation of outward K+ currents by membrane cholesterol content in rat left ventricular myocytes. Pflugers Arch 467:299-309 doi:10.1007/s00424-014-1521-3
9. Savio E, Goldhaber JI, Bridge JHB, Sachse FB (2007) A Framework for Analyzing Confocal Images of Transversal Tubules in Cardiomyocytes. In:Springer Berlin Heidelberg, Berlin, Heidelberg, p 110-119
10. Schindelin J, Arganda-Carreras I, Frise E, Kaynig V, Longair M, Pietzsch T, Preibisch S, Rueden C, Saalfeld S, Schmid B, Tinevez JY, White DJ, Hartenstein V, Eliceiri K, Tomancak P, Cardona A (2012) Fiji: an open-source platform for biological-image analysis. Nat Methods 9:676-682 doi:10.1038/nmeth.2019
11. Schwab BC, Seemann G, Lasher RA, Torres NS, Wulfers EM, Arp M, Carruth ED, Bridge JH, Sachse FB (2013) Quantitative analysis of cardiac tissue including fibroblasts using three-dimensional confocal microscopy and image reconstruction: towards a basis for electrophysiological modeling. IEEE Trans Med Imaging 32:862-872 doi:10.1109/TMI.2013.2240693
12. Seidel T, Dräbing T, Seemann G, Sachse FB (2013) A semi-automatic approach for segmentation of three-dimensional microscopic image stacks of cardiac tissue. Lecture Notes in Computer Science 7945:300-307
13. Seidel T, Edelmann JC, Sachse FB (2016) Analyzing Remodeling of Cardiac Tissue: A Comprehensive Approach Based on Confocal Microscopy and 3D Reconstructions. Ann Biomed Eng 44:1436-1448 doi:10.1007/s10439-015-1465-6
14. Seidel T, Navankasattusas S, Ahmad A, Diakos NA, Xu WD, Tristani-Firouzi M, Bonios MJ, Taleb I, Li DY, Selzman CH, Drakos SG, Sachse FB (2017) Sheet-

Like Remodeling of the Transverse Tubular System in Human Heart Failure Impairs Excitation-Contraction Coupling and Functional Recovery by Mechanical Unloading. Circulation 135:1632-1645 doi:10.1161/CIRCULATIONAHA.116.024470
15. Taylor SC, Posch A (2014) The design of a quantitative western blot experiment. Biomed Res Int 2014:361590 doi:10.1155/2014/361590
16. Wagner M, Rudakova E, Volk T (2008) Aldosterone-induced changes in the cardiac L-type Ca2+ current can be prevented by antioxidants in vitro and are absent in rats on low salt diet. Pflügers Archiv - European Journal of Physiology 457:339 doi:10.1007/s00424-008-0518-1